Advanced Materials Research *Online: 2014-08-11*
ISSN: 1662-8985, Vol. 996, pp 924-929
doi:10.4028/www.scientific.net/AMR.996.924

Microstresses in ZrO_2 layer and lateral cracking

BERDIN Clotilde[1,a *], TANG Yan[2,b] and PASCAL Serge[2,c]

[1] Univ. Paris-Sud, ICMMO/LEMHE UMR CNRS 8182, Bat 410, F-91405 Orsay cedex, France

[2] CEA Saclay, DEN, DM2S, SEMT, F-91191 Gif sur Yvette

[a] Clotilde.berdin@u-psud.fr, [b] xiaotyan6@gmail.fr, [c] serge.pascal@cea.fr

Keywords: oxide, internal stresses, finite element modeling, polycrystalline aggregate, damage.

Abstract. Micromechanical simulations of polycrystalline zirconia using the finite element method are performed in order to obtain the stresses at the grain scale of a zirconium oxide layer, since these microstresses are important for damage prediction of the layer and then oxidation kinetics. The crystallographic texture of the layer of monoclinic zirconia is taken into account. The results show that even under high compressive macroscopic stresses, the microstresses can contribute to lateral cracking promoted by the presence of tetragonal zirconia.

Introduction

Zirconium alloys used for the cladding of nuclear fuel are submitted to corrosion and a brittle zirconia layer develops on the cladding. It is well known that number of zirconium alloys present a breakaway of the oxidation kinetics that is associated to the development of lateral cracking within the oxide [1,2] with microcracks parallel to the metal-oxide interface. This damage is driven by the growth stresses. These stresses are mainly stemming from the change of the molar volume between the metal and the oxide which is characterized by the Pilling and Bedworth ratio (PBR). Since the PBR is about 1.5 for the Zr/ZrO_2 system, this induces high compressive stresses (around -1.5 GPa) [3,4] parallel to the metal/oxide interface. They could explain the presence of tetragonal zirconia (ZrO2t) at the interface, which transforms in monoclinic zirconia (ZrO2m) as oxide thickens [2,4,5].

The macroscopic stress state (1st order) can be obtained by experimental measurements. However, the microstresses (2^{nd} and 3^{rd} order) can play a role in the damage occurrence since brittle materials are sensitive to extreme values arising in the microstructure. The mean value of the stresses at the grain scale (2^{nd} order) could be assessed using mean field homogenization models. But, only full microstructure computations can provide the intra-granular stress distributions [6,7].

So, this work aims at using polycrystalline aggregate computations in elasticity with the finite element code Cast3M [8] in order to obtain the microstress distribution within a zirconia layer during the oxide growth. The first part is dedicated to the presentation of the microstructure computations; a comparison between full microstructure computations and results that could be obtained by the mean field theories of homogenization is presented. It is demonstrated that microstress distribution cannot accurately be obtained with mean field theories. So, in the second part, we use polycrystalline aggregate computations in order to obtain the microstress distribution arising during the oxide growth. The presence of tetragonal zirconia as an heterogeneity in the layer is studied and its influence on the lateral cracking is discussed.

Microstructure computations

Geometries and boundary conditions. Zirconia layer is a polycrystalline aggregate, so that strain incompatibilities arise between the grains that induce stress heterogeneities and play a role in the damage occurrence of the material. The finite element method allows computing microstresses due to the heterogeneity of the microstructure. The first approach consists in the study of a spherical heterogeneity embedded in the equivalent homogeneous medium (EHM). It is inspired from the

mean field theory of homogenization and the model is equivalent to the self-consistent one. The second approach uses a full description of the polycrystalline aggregate. A previous work [7] showed that a mesh with 512 grains is large enough to be a representative volume element, and the grain morphology has no effect on the microstress distribution; classical Voronoï tessellation is then used to obtain equiaxed grains.

Both geometries are unit cubes defined between (x=0, y=0, z=0) and (x=1, y=1, z=1); the spherical heterogeneity has a 0.2 radius. The unit cubes are meshed with linear tetrahedrons (Fig. 1). Kinematic uniform boundary conditions are applied in order to submit the unit cube to a simple extension in the ***x***-direction with a magnitude of ε_0=0.001 (see [7] for more details).

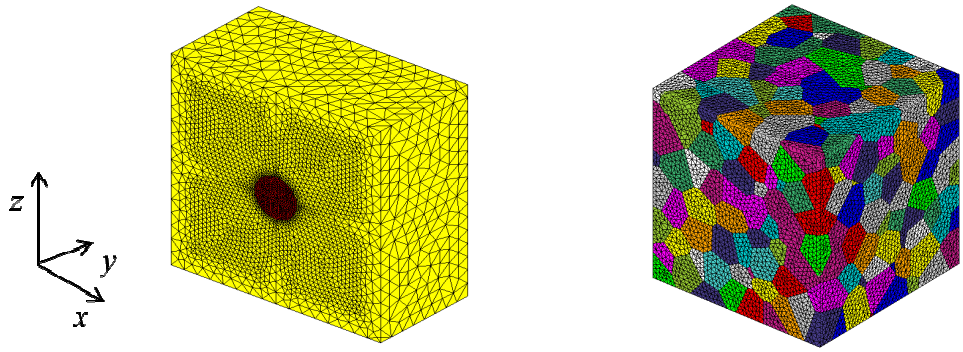

Fig. 1. Mesh of the heterogeneity within the homogeneous medium presented with a cut at y=0.5 (left); mesh of the polycristalline aggregate with 512 grains (right)

Mechanical properties. The heterogeneity within the EHM and each grain of the polycrystalline aggregate behaves as the crystal of ZrO2m with the elastic moduli given in Table 1. The polycrystalline aggregate is first considered as a linear elastic isotropic medium: the crystal orientations are then defined by 3 Euler angles obtained according to a Monte-Carlo process with a uniform distribution over the angle space. The properties of the isotropic EHM were derived from microstructure computations [7]: the elastic moduli are the average values between those obtained with kinematic uniform boundary conditions and with static uniform boundary conditions. They are given in Table 1.

Table 1. Moduli [GPa] of the monoclinic and tetragonal zirconia (ZrO2m, ZrO2t) and moduli computed for the polycrystalline monoclinic layer according to different crystallographic texture for ZrO2m: isotropic and with a ***z***=***c*** fiber texture (moduli are given in the frame of the material symmetry with the following Voigt notation: (1,2)=4, (1,3)=4, (2,3)=6 and $x \leftrightarrow 1$, $y \leftrightarrow 2$ $z \leftrightarrow 3$)

C_{IJ}	C_{11}	C_{12}	C_{13}	C_{15}	C_{22}	C_{23}	C_{25}	C_{33}	C_{35}	C_{44}	C_{46}	C_{55}	C_{66}
ZrO2m	358	144	67	-26	426	127	38	240	-23	130	-39	79	99
isotropic	319	115	115		319	115		319		102		102	102
z=***c***	385	147	95		385	95		233		119		83	83
ZrO2t	327	100	62		327	62		264		64		59	59

Results. In order to compare the second order stresses given by the both approaches, 500 different crystalline orientations have been considered for the modeling of the heterogeneity within the EHM; this is about the number of grains of the polycrystalline aggregate. Since the heterogeneity is spherical and the EHM is large enough to avoid boundary condition effects, the stress state within the heterogeneity is uniform. In the polycrystalline computation, the intragranular stress heterogeneity is obtained (Fig. 2 and 3). The average value of σ_{xx} within the heterogeneity or within each grain g of the polycristalline aggregate, $<\sigma_{xx}>_g$, is reported versus the elastic modulus of each grain (or heterogeneity) computed in the global frame, C_{11}^{xg} (Fig. 2). The Voigt solution (*i.e.* the strain is uniform over the RVE) leads to the result: $<\sigma_{xx}>_g = C_{11}^{xg}\varepsilon_0$ and is represented by a straight

line. The deviation of the result of the embedded heterogeneity from the Voigt solution stems from the interaction between each grain with the EHM, whereas the full microstructure computation takes also into account the interaction between the grains and their close neighborhood: a large spread is observed. One can conclude that mean field theories underestimate or overestimate the second order stress state at the crystalline scale. Furthermore, the comparison between Fig.2 and Fig.3 shows that the extreme values of the 3rd order of microstresses are different from those of 2nd order.

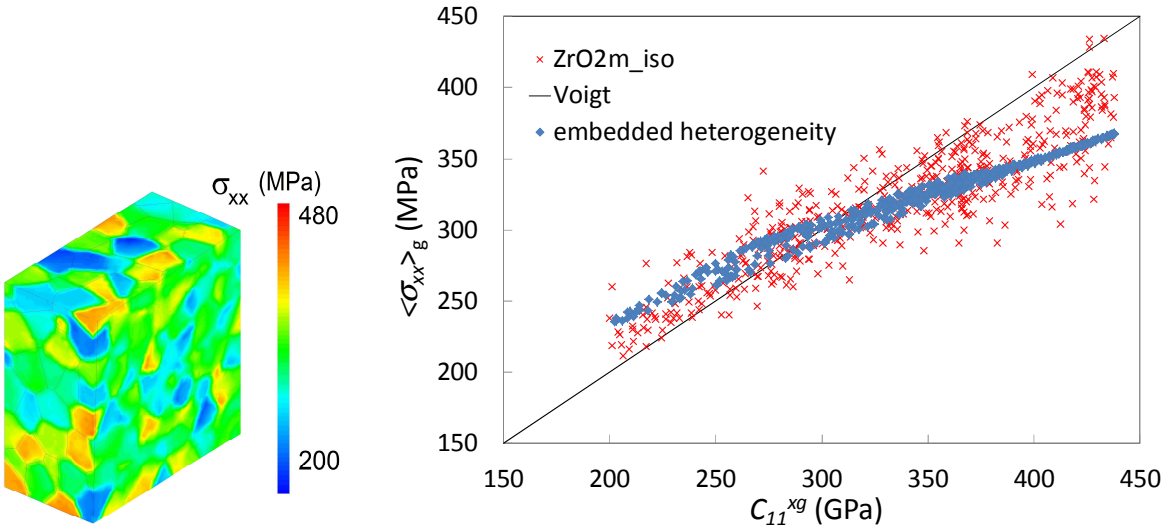

Fig. 2. Simple extension in ***x***-direction (ε_0=0.001) for the isotropic polycrystal; isocontours of σ_{xx} in the polycrystalline aggregate (left); average value of σ_{xx} over each grain *g* or heterogeneity versus the elastic modulus C_{11}^{xg} of the grain, computed in the global frame of the RVE (right).

Zirconia layer presents a crystallographic texture [2,4,9]; Parise et al. [9] found a fiber texture with the ***c*** axis of the monoclinic unit cell parallel to the ***z*** axis, that is normal to the metal-oxide interface. So, this fiber texture must be taken into account in the aggregate modeling: the crystalline orientation of each grain is defined by one angle around the ***c*** axis. This fiber texture induces a higher mean value of the stress σ_{xx} and a lower standard deviation than the isotropic case (Fig. 3): the higher mean value is related to the higher elastic moduli in this direction as can be seen in the Table 3, and the lower standard deviation is explained by the small number of different crystalline orientations in comparison with the isotropic case.

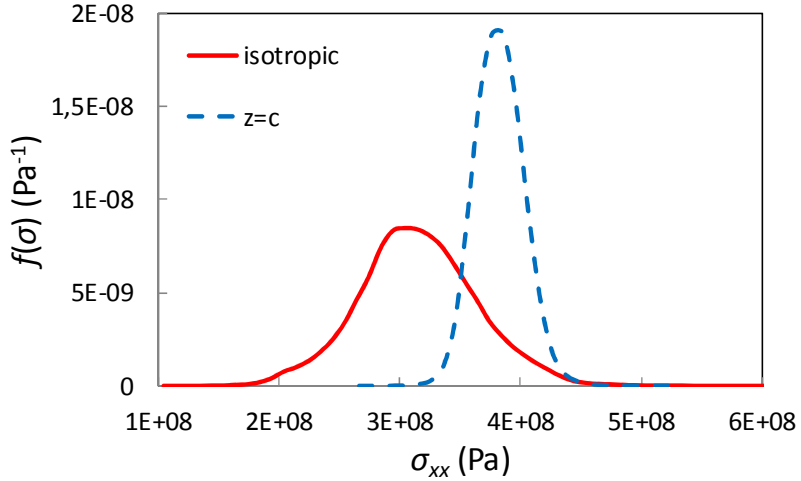

Fig. 3. Distribution density of σ_{xx} for an extension in the ***x***-direction for an aggregate whether isotropic or textured (***z***=***c*** ideal fiber texture)

Microstresses within the oxide layer

Macroscopic loading. During the oxide growth, internal stresses develop due to the molar volume change between the metal and the oxide, and other phase transformations such as tetragonal to monoclinic zirconia. These transformations induce strains, $\varepsilon_{ij}^{\mathrm{tr}}$, within the oxide that are constrained by the metal. Considering a thin layer, analytical computations allow to obtain the macroscopic mechanical stress state within the substrate and the layer. So, an equibiaxial stress state can be assumed in the interface plane (***x***, ***y***) and the following equations are used to compute the mechanical stress state at the macroscopic scale:

$$\varepsilon_{xx}^{ox} = \varepsilon_{xx}^{m} \quad \sigma_{xx}^{ox} h_{ox} + \sigma_{xx}^{m} h_m = 0 \tag{1}$$

$$\varepsilon_{xx}^{ox} = \frac{1+\nu_{xy}^{ox}}{E_x^{ox}} \sigma_{xx}^{ox} + \varepsilon_{xx}^{tr} \qquad \varepsilon_{xx}^{m} = \frac{1+\nu^{m}}{E^{m}} \sigma_{xx}^{m} \tag{2}$$

with $\varepsilon_{xx}^{ox}, \varepsilon_{xx}^{m}$ the strains in the oxide and in the metal, $\sigma_{xx}^{ox}, \sigma_{xx}^{m}$ the stresses in the oxide and in the metal, h_{ox}, h_m the thickness of the oxide and that of the metal, ε_{xx}^{tr} the transformation strain that appears only within the oxide, E_x^{ox}, ν_{xy}^{ox}, E^m, ν^m, the elastic properties of the oxide and that of the metal. The elastic properties of the oxide are computed from the elastic moduli obtained from microstructure computations for the fiber texture ***z***=***c*** with kinematic uniform boundary conditions (see Table 1), and the elastic properties of isotropic zirconium are used for the metal (E^m =80 GPa, ν^m =0.3).

An assessment of the transformation strains was proposed by Parise et al. [9] for a zirconia layer growing on Zr, in the ***z***-direction with a fiber texture ***z***=***c***. The strain transformation tensor is such that the result of a deflection test is recovered and the volume change satisfies the PBR: $\varepsilon_{xx}^{tr} = \varepsilon_{yy}^{tr}$ =0.005, $(1+\varepsilon_{xx}^{tr})^2(1+\varepsilon_{zz}^{tr})$=PBR.

For the numerical application, the value of the oxide thickness is chosen in the range of thickness for which the lateral cracking occurs [2]: h_{ox}=1.4 μm. Solving the previous equation system with h_m=400 μm, which is the typical thickness of nuclear fuel cladding and sheets used for oxidation studies [9], the stress in the oxide is: σ_{xx}^{ox} =-2266 MPa, related to a total strain: ε_{xx}^{ox} =-5.019 10^{-3}.

So, in order to compute the microstresses within the oxide due to the macroscopic mechanical state that develops during the oxide growth, the following boundary conditions are prescribed on the RVE with 512 grains: for the nodes with the coordinates x=0: u_x=0, for the nodes at y=0; u_y=0, for the nodes at z=0: u_z=0, for the nodes at x=1: u_x =-5.019 10^{-3} and for the nodes located at y=1: u_y=-5.019 10^{-3}. It is recalled that there is no absolute dimension in this problem, and no unit is defined for the coordinates, neither for the displacements. Finally, the face z=1 is free. It should be noted that the polycrystalline aggregate only represents a part of the ZrO2m layer.

Results. The isocontours of σ_{xx} and σ_{zz} are reported at the Fig. 4. The normal stress in the ***x***-direction varies from grain to grain as in the case of the extension in the ***x***-direction. The mean value is very close to -2266 MPa as expected. It should be noted that extreme values arises at the boundaries due the prescribed conditions: they are not really representative of the values inside the polycrystal; this effect is also noticeable in the Fig. 2. So, such type of results should always be presented with a cut of the RVE. The normal stress to the ***z***-direction corresponds to the normal stress that can trigger the lateral microcracks if the stress is positive. The mean value of σ_{zz} is zero as expected, but there are grains that are submitted to tension in ***z***-direction. This can play a role in the damage occurrence.

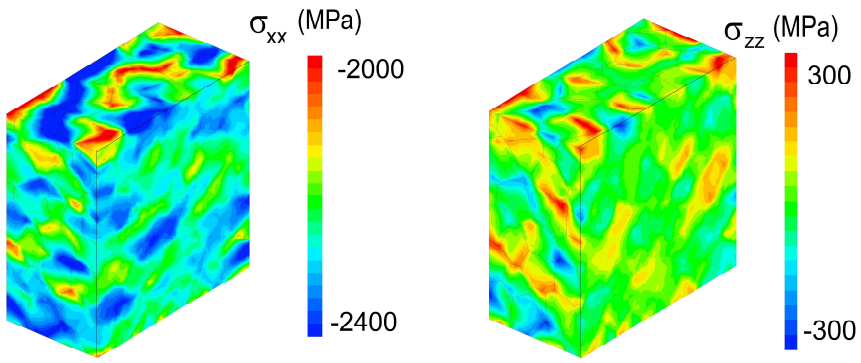

Fig. 4. Microstresses due to growth stresses within an aggregate of ZrO2m cut by the plane x=0.5; σ_{xx} isocontours (left) and σ_{zz} isocontours (right)

Influence of the presence of tetragonal zirconia within the layer. Number of studies reports the presence of a tetragonal ZrO_2 phase (ZrO2t) within the oxide of Zr alloys, even at moderate temperatures [2,4,5]. The volume fraction on ZrO2t decreases with the increase of the thickness and is mainly located at the interface with the metal.

So, the microstresses are computed taking into account this phase as an heterogeneity (no pahse transformation is taken into account): the grains located at a distance greater than or equal to 0.3 from the bottom of the unit cube have the mechanical properties and the crystallographic orientation of the monoclinic zirconia as defined in the previous subsection; but the grains located at a distance lower than 0.3 have the mechanical properties of tetragonal zirconia (see Table 1), and their orientation is randomly distributed such that the tetragonal layer has an isotropic behavior. As a matter of fact, the tetragonal layer has probably a crystallographic texture as mentioned in papers [2,5], but the anisotropy of the tetragonal phase is low and a crystallographic texture does not induce a large modification of the properties of the layer.

The boundary conditions defined in the previous subsection are applied: the polycrystalline aggregate is submitted to a macroscopic loading that corresponds to a layer of 1.4 µm thickness over a zirconium substrate of 400 µm thickness, considering that the layer of ZrO2t is too thin to modify this result. As in the previous case, it should be noted that the polycrystalline aggregate only represents a part of the ZrO2 layer containing both zirconia phases; the relative fraction of ZrO2t (0.3) was not representative of the full tetragonal fraction in the layer, but it was chosen in order to avoid the boundary conditions effects on the computed stresses. The isocontours of σ_{xx} and σ_{zz} are reported in the Fig. 5.

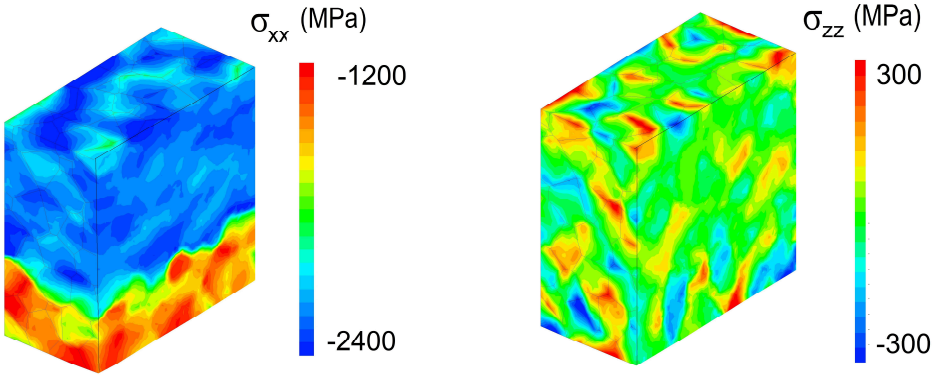

Fig. 5. Microstresses due to growth stresses within an aggregate of zirconia containing 30% of ZrO2t and cut by the plane at x=0.5; σ_{xx} isocontours (left) and σ_{zz} isocontours (right).

The normal stress in the ***x***-direction is about -2200 MPa as in the previous case whereas the value in the tetragonal phase is about -1300 MPa because of lower elastic moduli of ZrO2t. The isocontours of the stress normal to the interface, σ_{zz}, is not so different than those of the full

monoclinic aggregate; however, it can be seen that the higher values are located within the tetragonal phase or at the interface between both zirconia phases. This observation is not induced by particular misorientations of grains and has been verified with other computations with other crystalline orientations.

So, the presence of a layer of tetragonal phase increases the microstress heterogeneity and can promote lateral microcracking. It is worth noting that such microcracks are noted near the tetragonal phase in [2].

Concluding remarks

Two types of microstructure computations were performed with the finite element method in order to obtain the microstresses within a zirconia layer growing on Zr during oxidation: 1) spherical heterogeneity embedded in the homogeneous equivalent material and 2) polycrystalline aggregate taking into account each grain of the polycrystal. The computations show that the influence of the close neighborhood induces a large scatter around the average microstresses within the grains that is not taken into account by the mean field theories of homogenization. Crystallographic texture modifies the microstress distribution and has to be taken into account.

The macroscopic loading of a textured oxide that grows on Zr substrates was assessed by analytical formulas in the linear elasticity framework. The phase transformation (from metal to oxide) was represented by a uniform strain tensor proposed in the literature: a high level of equibiaxial compressive stress state within the oxide layer was found. The polycrystalline aggregate was submitted to this macroscopic loading. The polycrystalline heterogeneity induces regions with tensile stress that can trigger lateral microcrack. This effect is reinforced by the presence of a tetragonal zirconia in the oxide layer.

References

[1] P. Bossis, F. Lefebvre, P. Barberis, A. Galerie, Corrosion of zirconium alloys, Mat. Sc. For 369-371 (2001) 255-262.

[2] A. Ylmazbayhan, E. Breval, A.T. Motta, R.J. Comstock, Transmission electron microscopy examination of oxide layers formed on Zr alloys, J. Nuc. Mat. 349 (2006) 265-281.

[3] C. Roy, B. Burgess, A study of the stresses generated in zirconia films during the oxidation of zirconium alloys, Ox. Metals 2 (1970) 235-261.

[4] N. Pétigny, P. Barberis, C. Lemaignan, C. Valot, M. Lallemant, In situ XRD analysis of the oxide layers formed by oxidation at 743 K on Zy4 an Zr-1NbO, J. Nuc. Mat. 280 (2000) 318-330.

[5] J. Lin, H. Li, C Nam, J.A. Szpunar, Analysis on volume fraction and crystal orientation relationship of monoclinic and tetragonal oxide grown on Zr-2.5Nb alloy, J. Nuc. Mat. 334 (2004) 200-206.

[6] G. Cailletaud, S. Forest, D. Jeulin, F. Feyel, I. Galliet, V. Mounoury, S. Quilici, Some elements of microstructural mechanics, Comp. Mat. Sc. 27 (2003) 351–374.

[7] C. Berdin, Z. Y. Yao, S. Pascal, Internal stresses in polycrystalline zirconia: microstructure effects, Comp. Mat. Sc. 70 (2013) 140-144.

[8] CEA, DEN, DM2S, SEMT, Cast3M, http://www-cast3m.cea.fr/

[9] M. Parise, O. Sicardy, G. Cailletaud, Modelling of the mechanical behavior of the metal-oxide system during Zr alloy oxidation, J. Nuc. Mat. 256 (1998) 35-46.